

Stellar origin of the ^{182}Hf cosmochronometer and the presolar history of solar system matter

Maria Lugaro,^{1*} Alexander Heger,^{1,2,3} Dean Osrin,¹
Stephane Goriely,⁴ Kai Zuber,⁵ Amanda I. Karakas,⁶
Brad K. Gibson,^{7,8,9} Carolyn L. Doherty,¹ John C. Lattanzio,¹
Ulrich Ott¹⁰

¹Monash Centre for Astrophysics (MoCA), Monash University,
Clayton VIC 3800, Australia

²Joint Institute for Nuclear Astrophysics (JINA)

³School of Physics and Astronomy, University of Minnesota,
Minneapolis, MN 55455, USA

⁴Institut d'Astronomie et d'Astrophysique, Université Libre de Bruxelles,
CP-226, 1050, Brussels, Belgium

⁵Institut für Kern- und Teilchenphysik, Technische Universität Dresden,
01069 Dresden, Germany

⁶Research School of Astronomy and Astrophysics, Australian National University,
Canberra, ACT 2611, Australia

⁷Jeremiah Horrocks Institute, University of Central Lancashire,
Preston, PR1 2HE, United Kingdom

⁸Institute for Computational Astrophysics, Department of Astronomy & Physics,
Saint Mary's University, Halifax, NS, BH3 3C3, Canada

⁹UK Network for Bridging Disciplines of Galactic Chemical Evolution (BRIDGCE)

¹⁰Faculty of Natural Science, University of West Hungary,
9700 Szombathely, Hungary

*To whom correspondence should be addressed; E-mail: maria.lugaro@monash.edu.

Among the short-lived radioactive nuclei inferred to be present in the early

solar system via meteoritic analyses there are several heavier than iron whose stellar origin has been poorly understood. In particular, the abundances inferred for ^{182}Hf (half-life = 8.9 Myr) and ^{129}I (half-life = 15.7 Myr) are in disagreement with each other if both nuclei are produced by the rapid neutron-capture process. Here we demonstrate that, contrary to previous assumption, the slow neutron-capture process in asymptotic giant branch stars produces ^{182}Hf . This has allowed us to date the last rapid and slow neutron-capture events that contaminated the solar system material at ~ 100 Myr and ~ 30 Myr, respectively, before the formation of the Sun.

Radioactivity is a powerful clock for measuring cosmic times. It has provided us the age of the Earth[1], the ages of old stars in the halo of our Galaxy[2], the age of the solar system[3, 4], and a detailed chronometry of planetary growth in the early solar system[5]. The exploitation of radioactivity to measure timescales related to the presolar history of the solar system material, however, has been so far hindered by our poor knowledge of how radioactive nuclei are produced by stars. Of particular interest are three radioactive isotopes heavier than iron: ^{107}Pd , ^{129}I , and ^{182}Hf , with half-lives of 6.5 Myr, 15.7 Myr, and 8.9 Myr, respectively, and initial abundances (relative to a stable isotope of the same element) in the early solar system of $^{107}\text{Pd}/^{108}\text{Pd} = 5.9 \pm 2.2 \times 10^{-5}$ [6], $^{129}\text{I}/^{127}\text{I} = 1.19 \pm 0.20 \times 10^{-4}$ [7], and $^{182}\text{Hf}/^{180}\text{Hf} = 9.72 \pm 0.44 \times 10^{-5}$ [8]. The current paradigm is that ^{129}I and ^{182}Hf are mostly produced by rapid neutron captures (the r process), where the neutron density is relatively high ($> 10^{20} \text{ cm}^{-3}$) resulting in much shorter time-scales for neutron capture than β -decay[9]. The r process is believed to occur in neutron star mergers or peculiar supernova environments[10, 11]. Additionally to the r process, ^{107}Pd is also produced by slow neutron captures (the s process), where the neutron density is relatively low ($< 10^{13} \text{ cm}^{-3}$) resulting in shorter time-scales for β -decay than neutron capture, the details depending on the β -decay rate of each unstable isotope and the local neutron

density[9]. The main site of production of the s -process elements from Sr to Pb in the Galaxy is in asymptotic giant branch (AGB) stars[12], the final evolutionary phase of stars with initial mass lower than ~ 10 solar masses (M_{\odot}). Models of the s process in AGB stars have predicted marginal production of ^{182}Hf [13] because the β -decay rate of the unstable isotope ^{181}Hf at stellar temperatures was estimated to be much faster [14] than the rate of neutron capture leading to the production of ^{182}Hf (Fig. 1).

Uniform production of ^{182}Hf and ^{129}I by the r process in the Galaxy, however, cannot self-consistently explain their meteoritic abundances[15, 16, 17]. The simplest equation for uniform production (hereafter UP) of the abundance of a radioactive isotope in the Galaxy, relative to a stable isotope of the same element produced by the same process, is given by

$$\frac{N_{radio}}{N_{stable}} = \frac{P_{radio}}{P_{stable}} \times \frac{\tau}{T}, \quad (1)$$

where N_{radio} and N_{stable} are the abundances of the radioactive and stable isotopes, respectively, P_{radio}/P_{stable} is the ratio of their stellar production rates, τ is the mean lifetime of the radioactive isotope, and $T \sim 10^{10}$ yr is the timescale of the evolution of the Galaxy. Some time during its presolar history, the solar system matter became isolated from the interstellar medium characterised by UP abundance ratios. Assuming that both ^{129}I and ^{182}Hf are primarily produced by the r process, one obtains inconsistent isolation times using $^{129}\text{I}/^{127}\text{I}$ or $^{182}\text{Hf}/^{180}\text{Hf}$: 72 Myr or 15 Myr, respectively, prior to the solar system formation[17]. This conundrum led Wasserburg *et al.*[15] to hypothesise the existence of two types of r -process events. Another proposed solution is that the ^{107}Pd , ^{129}I , and ^{182}Hf present in the early solar system were produced by the neutron burst that occurs during core-collapse supernovae[18, 19, 20]. This does not result in elemental production, but the relative isotopic abundances of each element are strongly modified due to relatively high neutron densities with values between those of the s and r processes.

We have updated model predictions of the production of ^{182}Hf and other short-lived radioa-

tive nuclei in stars of initial masses between $1.25 M_{\odot}$ and $25 M_{\odot}$ (Table S1). Stars of initial mass up to $8.5 M_{\odot}$ evolve onto the AGB phase and have been computed using the Monash code[21, 22, 23, 24]. Stars of higher mass evolve into core-collapse supernovae and have been computed using the KEPLER code[25, 26]. The estimates of β -decay rates by Takahashi & Yokoi[14] were based on nuclear level information from the Table of Isotopes (ToI) database, which included states for ^{181}Hf at 68 keV, 170 keV, and 298 keV. The 68 keV level was found to be responsible for a strong enhancement of the β -decay rate of ^{181}Hf at s -process temperatures, preventing the production of ^{182}Hf during the s process (Fig. 1). More recent experimental evaluations[27], however, did not find any evidence for the existence of these states. Removing them from the computation of the half-life of ^{181}Hf in stellar conditions results in values compatible with no temperature dependence for this isotope (Fig. S2), within the uncertainties.

The removal of the temperature dependence of the β -decay rate of ^{181}Hf resulted in an increase by a factor of 4 – 6 of the ^{182}Hf abundance predicted by the AGB s -process models. The effect was milder on the predictions from the supernova neutron burst, with increases between 7% for the $15 M_{\odot}$ model and up to a factor of 2.6 for the $25 M_{\odot}$ model. Some production of ^{182}Hf , as well as of ^{129}I and ^{107}Pd , is achieved in all the models, with $^{182}\text{Hf}/^{180}\text{Hf}$ ranging from ~ 0.001 to ~ 0.3 (Fig. 2). In terms of the absolute ^{182}Hf abundance, however, only AGB models of mass $\sim 2 - 4 M_{\odot}$ are major producers of s -process ^{182}Hf in the Galaxy, due to the combined effect of the $^{13}\text{C}(\alpha, n)^{16}\text{O}$ and the $^{22}\text{Ne}(\alpha, n)^{25}\text{Mg}$ neutron sources[22, 20]. Only in these stars in fact the production factor of the stable ^{180}Hf with respect to its solar value is well above unity.

When using Eq. 1 with the updated $s+r$ production rate ratio for $^{182}\text{Hf}/^{180}\text{Hf}$, we still have the problem that the time of isolation of the solar system material from the average interstellar medium is much shorter than the value obtained using $^{129}\text{I}/^{127}\text{I}$ (Table 1). For the nuclei under consideration, however, it is likely that their mean lifetimes are smaller or similar to the recurrence time, δ , between the events that produce them. In this case, the granularity of the

production events controls the abundances and the correct scaling factor for the production ratio is the number of events, T/δ . Because the cosmic abundances of these nuclei result from two different types of sources, the r process and the s process, it necessarily follows that the precursor material of the solar system must have seen a last event (LE) of each type, i.e., a r -process LE and a s -process LE. Following each of these LE, the abundance of a radioactive isotope in the Galaxy, relatively to a stable isotope of the same element produced by the same process, is given by:

$$\frac{N_{radio}}{N_{stable}} = \frac{p_{radio}}{p_{stable}} \times \frac{\delta}{T} \times \left(1 + \frac{e^{-\delta/\tau}}{1 - e^{-\delta/\tau}} \right), \quad (2)$$

where p_{radio}/p_{stable} are the production ratio of each single stellar event and the second term of the sum accounts for the memory of all the previous events[16]. Employing simple considerations on the expansion of stellar ejecta into the interstellar medium and the resulting contamination of the Galactic disk [18] one can derive $\delta \sim 10$ Myr for supernovae and ~ 50 Myr for AGB stars in the mass range $2 - 4 M_{\odot}$. Because these values are first approximations, and because the r process probably does not occur in every supernova, in Table 1 we present the results obtained using $\delta = 10 - 100$ Myr. The time of the r -process LE as derived from $^{129}\text{I}/^{127}\text{I}$ is $80 - 109$ Myr (Table 1), in agreement (within the uncertainties) with the $95 - 123$ Myr values derived from the early solar system $^{247}\text{Cm}/^{235}\text{U}$ ratio, which can only be produced by the r process and whose initial abundance needs confirmation. This r -process LE time is in strong disagreement with the r -process LE times derived from $^{107}\text{Pd}/^{108}\text{Pd}$ and $^{182}\text{Hf}/^{180}\text{Hf}$, which should be considered upper limits, given that the abundances of ^{108}Pd and ^{180}Hf have an important (70% to 80%) s -process contribution that is not accounted for when considering r -process events only. A natural explanation is to invoke a separate s -process LE for ^{107}Pd and ^{182}Hf . When calculating the time of this event under the approximation that the stable reference isotopes ^{108}Pd and ^{180}Hf are of s -process origin, which is correct within 30%, we derive concordant times from ^{107}Pd and ^{182}Hf of $\sim 10 - 30$ Myr (Table 1). Our derived timeline for the solar system formation is

schematically drawn in Fig. 3.

Our timing of the *s*-process LE that contributed the final addition of elements heavier than Fe to the precursor material of the solar system has implications for our understanding of the events that led to the formation of the Sun. This is because it provides us with an upper limit of the time prior to the solar system formation when the precursor material of the solar system became isolated from the ongoing chemical enrichment of the Galaxy. This isolation timescale can represent the time it took to form the giant molecular cloud where the proto-solar molecular cloud core formed, plus the time it took to form and collapse the proto-solar cloud core itself. Interestingly, it compares well to the total lifetime (from formation to dispersal) of typical giant molecular clouds of 27 ± 12 Myr[28]. In this context, other radioactive nuclei in the early solar system of possible stellar origin (Table S2), e.g., ^{26}Al , probably result from self-pollution of the star-forming region itself[29, 30, 31, 20]. This is not possible for the radioactive nuclei of *s*-process origin considered here, because their $\sim 3 M_{\odot}$ parent stars live too long (~ 400 Myr) to evolve within star-forming regions. Our present scenario implies that the origin of ^{26}Al and ^{182}Hf in the early solar system was decoupled, in agreement with recent meteoritic analysis, which have demonstrated the presence of ^{182}Hf in an early solar system solid that did not contain ^{26}Al [32].

References and Notes

- [1] S. A. Wilde, J. W. Valley, W. H. Peck, C. M. Graham, *Nature* **409**, 175 (2001).
- [2] A. Frebel, *et al.*, *Astrophys. J.* **660**, L117 (2007).
- [3] Y. Amelin, *et al.*, *Earth and Planetary Science Letters* **300**, 343 (2010).
- [4] J. N. Connelly, *et al.*, *Science* **338**, 651 (2012).

- [5] N. Dauphas, M. Chaussidon, *Annu. Rev. Earth Planet. Sci.* **39**, 351 (2011).
- [6] M. Schönbächler, R. W. Carlson, M. F. Horan, T. D. Mock, E. H. Hauri, *Geochim. Cosmochim. Acta* **72**, 5330 (2008).
- [7] R. H. Brazzle, O. V. Pravdivtseva, A. P. Meshik, C. M. Hohenberg, *Geochim. Cosmochim. Acta* **63**, 739 (1999).
- [8] C. Burkhardt, *et al.*, *Geochim. Cosmochim. Acta* **72**, 6177 (2008).
- [9] E. M. Burbidge, G. R. Burbidge, W. A. Fowler, F. Hoyle, *Rev. Mod. Phys.* **29**, 547 (1957).
- [10] M. Arnould, S. Goriely, K. Takahashi, *Phys. Rep.* **450**, 97 (2007).
- [11] F.-K. Thielemann, *et al.*, *Prog. Part. Nucl. Phys.* **66**, 346 (2011).
- [12] M. Busso, R. Gallino, G. J. Wasserburg, *Ann. Rev. Astron. Astrophys.* **37**, 239 (1999).
- [13] G. J. Wasserburg, M. Busso, R. Gallino, C. M. Raiteri, *Astrophys. J.* **424**, 412 (1994).
- [14] K. Takahashi, K. Yokoi, *At. Data Nucl. Data Tables* **36**, 375 (1987).
- [15] G. J. Wasserburg, M. Busso, R. Gallino, *Astrophys. J.* **466**, L109 (1996).
- [16] G. J. Wasserburg, M. Busso, R. Gallino, K. M. Nollett, *Nucl. Phys. A* **777**, 5 (2006).
- [17] U. Ott, K.-L. Kratz, *New Astron. Rev.* **52**, 396 (2008).
- [18] B. S. Meyer, D. D. Clayton, *Space Sci. Rev.* **92**, 133 (2000).
- [19] B. S. Meyer, *Chondrites and the Protoplanetary Disk*, A. N. Krot, E. R. D. Scott, B. Reipurth, eds. (2005), vol. 341 of *Astronomical Society of the Pacific Conference Series*, p. 515.

- [20] See supplementary online text for further discussion.
- [21] A. I. Karakas, D. A. García-Hernández, M. Lugaro, *Astrophys. J.* **751**, 8 (2012).
- [22] M. Lugaro, *et al.*, *Astrophys. J.* **780**, 95 (2014).
- [23] M. Lugaro, *et al.*, *Meteorit. Planet. Sci* **47**, 1998 (2012).
- [24] C. L. Doherty, P. Gil-Pons, H. H. B. Lau, J. C. Lattanzio, L. Siess, *Mon. Not. R. Astron. Soc.* **437**, 195 (2014).
- [25] T. Rauscher, A. Heger, R. D. Hoffman, S. E. Woosley, *Astrophys. J.* **576**, 323 (2002).
- [26] A. Heger, S. E. Woosley, *Astrophys. J.* **724**, 341 (2010).
- [27] V. Bondarenko, *et al.*, *Nucl. Phys. A* **709**, 3 (2002).
- [28] N. Murray, *Astrophys. J.* **729**, 133 (2011).
- [29] M. Gounelle, G. Meynet, *Astron. Astrophys.* **545**, A4 (2012).
- [30] A. Vasileiadis, Å. Nordlund, M. Bizzarro, *Astrophys. J.* **769**, L8 (2013).
- [31] E. D. Young, *Earth Planet. Sci. Lett.* **392**, 16 (2014).
- [32] J. C. Holst, *et al.*, *Proc. Natl. Acad. Sci. USA* **110**, 88198823 (2013).
- [33] G. A. Brennecka, *et al.*, *Science* **327**, 449 (2010).
- [34] M. Asplund, N. Grevesse, A. J. Sauval, P. Scott, *Ann. Rev. Astron. Astrophys.* **47**, 481 (2009).
35. J. M. Trigo-Rodríguez, *et al.*, *Meteorit. Planet. Sci* **44**, 627 (2009).
36. A. Takigawa, *et al.*, *Astrophys. J.* **688**, 1382 (2008).

37. A. N. Krot, *et al.*, *Astrophys. J.* **672**, 713 (2008).
38. K. Makide, *et al.*, *Astrophys. J.* **733**, L31 (2011).
39. C. Vockenhuber, *et al.*, *Phys. Rev. C* **75**, 015804 (2007).
40. K. Wisshak, *et al.*, *Phys. Rev. C* **73**, 045807 (2006).
41. C. Arlandini, *et al.*, *Astrophys. J.* **525**, 886 (1999).
42. S. Goriely, *Astron. Astrophys.* **342**, 881 (1999).
43. J. N. Ávila, *et al.*, *Astrophys. J.* **744**, 49 (2012).
44. T. Rauscher, *Astrophys. J.* **755**, L10 (2012).
45. M.-C. Liu, M. Chaussidon, G. Srinivasan, K. D. McKeegan, *Astrophys. J.* **761**, 137 (2012).
46. R. Mishra, M. Chaussidon, K. Marhas, *Proceedings of Science (NIC XII)085* (2012).

Acknowledgements We thank Martin Asplund for providing us updated early solar system abundances, Daniel Price and Christoph Federrath for comments, and Marco Pignatari for discussion. The data described in the paper are presented in Fig. S2 and Table S1. M.L., A.H., and A.I.K. are ARC Future Fellows on projects FT100100305, FT120100363, and FT10100475, respectively. This research was partly supported under Australian Research Council's Discovery Projects funding scheme (project numbers DP0877317, DP1095368 and DP120101815). U.O. thanks the Max Planck Institute for Chemistry for use of its IT facilities.

Supplementary Materials

www.sciencemag.org

Supplementary text

Figs. S1 and S2

Tables S1 and S2

References (35-46)

Ratio	P_{radio}/P_{stable}	UP ratio	UP time (Myr)	p_{radio}/p_{stable}	LE ratio	LE time [δ] (Myr)
$^{247}\text{Cm}/^{235}\text{U}$	0.40	8.8×10^{-3}	90	0.40(<i>r</i>)	3.8×10^{-2}	123[100]
					1.1×10^{-2}	95[10]
$^{129}\text{I}/^{127}\text{I}$	1.25	2.9×10^{-3}	73	1.35(<i>r</i>)	1.4×10^{-2}	109[100]
					3.8×10^{-3}	80[10]
$^{182}\text{Hf}/^{180}\text{Hf}$	0.29	3.8×10^{-4}	18	0.91(<i>r</i>)	9.1×10^{-3}	59[100]
					1.7×10^{-3}	37[10]
				0.15(<i>s</i>)	1.5×10^{-3}	36[100]
					2.8×10^{-4}	14[10]
$^{107}\text{Pd}/^{108}\text{Pd}$	0.65	6.1×10^{-4}	22	2.09(<i>r</i>)	2.1×10^{-2}	55[100]
					3.2×10^{-3}	38[10]
				0.14(<i>s</i>)	1.4×10^{-3}	30[100]
					2.1×10^{-4}	12[10]

Table 1: Production ratios and inferred timescales. P_{radio}/P_{stable} are the ratios of the stellar production rates (*s+r* processes), p_{radio}/p_{stable} are the production ratios of each single stellar event (*s* or *r* process, as indicated). The UP and LE ratios are calculated using Eq. 1 and Eq. 2, respectively. For $^{247}\text{Cm}/^{235}\text{U}$ in Eq. 1, T is substituted with the mean lifetime of ^{235}U ($\tau=1020$ Myr), and in Eq. 2, δ/T is removed and p_{radio}/p_{stable} is multiplied by the ratio of the summation terms derived for ^{247}Cm and for ^{235}U . The UP and LE times are the time intervals required to obtain the initial solar system ratio starting from the UP and LE ratios, respectively. For the initial $^{247}\text{Cm}/^{235}\text{U}$ we assume the average of the range given by Brennecka *et al.*[33] = $(1.1 - 2.4) \times 10^{-4}$. Meteoritic and nuclear uncertainties result in error bars on the reported times of the order of 10 Myr [20].

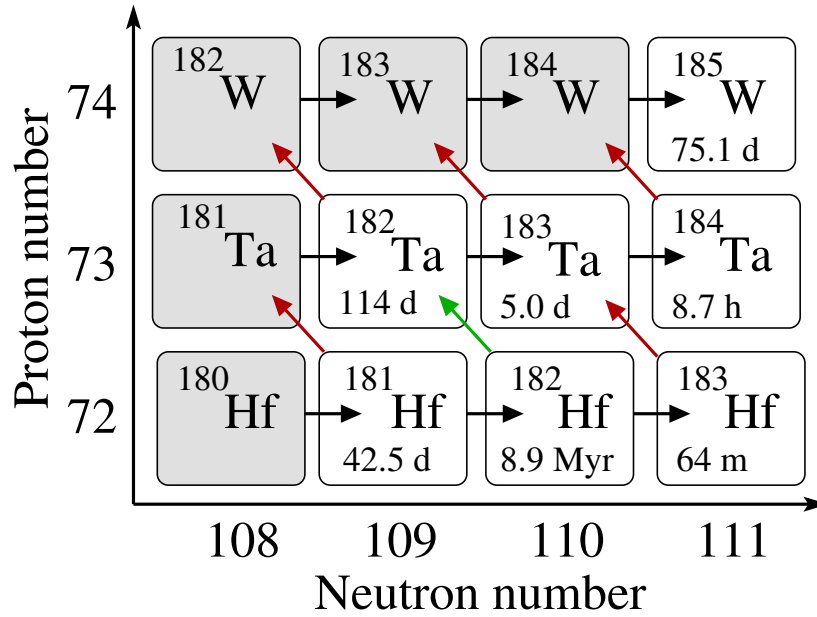


Figure 1: Section of the nuclide chart including Hf, Ta, and W, showing stable isotopes as grey boxes and unstable isotopes as white boxes (with their terrestrial half-lives). Neutron-capture reactions are represented as black arrows, β -decay as red arrows, and the radiogenic β -decay of ^{182}Hf as a green arrow. The production of ^{182}Hf is controlled by the half-life of the unstable ^{181}Hf , which precedes ^{182}Hf in the *s*-process neutron-capture isotopic chain. The probability of ^{181}Hf to capture a neutron to produce ^{182}Hf is $> 50\%$ for neutron densities $> 4 \times 10^9 \text{ cm}^{-3}$ or $> 10^{11} \text{ cm}^{-3}$, using a β -decay rate of 42.5 days (terrestrial) or of 30 hours at 300 million K, as according to Takahashi & Yokoi[14], respectively.

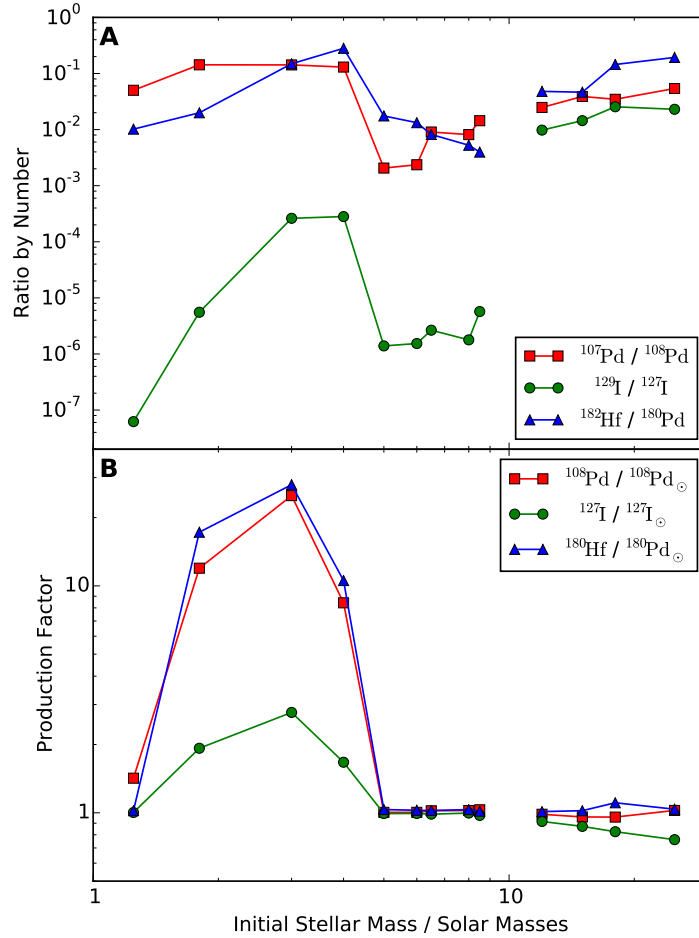


Figure 2: Stellar model predictions as function of the initial stellar mass. The production ratios of the radioactive isotopes of interest with respect to the stable reference isotope of the same element are shown in panel A, the production factors with respect to the initial solar composition of each stable reference isotope are shown in panel B. Stars below $10 M_\odot$ evolve through the AGB phase and associated s process, while stars above $10 M_\odot$ evolve through a core-collapse supernova and associated neutron burst. All the models were calculated using no temperature dependence for the half-life of ^{181}Hf and with initial solar abundances updated from Asplund *et al.*[34], corresponding to a metallicity 0.014.

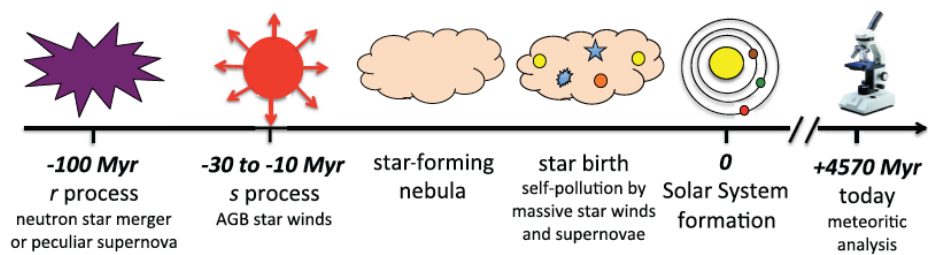


Figure 3: Schematic timeline of the solar system formation. The *r*-process LE contributed ^{129}I to the early solar system, the *s*-process LE ^{107}Pd and ^{182}Hf , and self-pollution of the star-forming region the lighter, shorter lived radionuclides, e.g., ^{26}Al .

Supplementary text

Pollution by injection from a single stellar source

A single local stellar polluter has been traditionally invoked to have possibly injected most of the radioactive isotopes into the early solar system (16, 19) and we briefly discuss here this scenario in the light of our models. In a simple pollution mixing model we have two free parameters: the dilution factor f of the stellar ejecta into the original pre-solar cloud, which is related to the distance of the polluter, and the time delay Δt between ejection of the radioactive isotopes from the star and the formation of the first solids in the solar system (16, 19, 23). We set these two parameters to match the abundances of ^{26}Al and ^{41}Ca and plot the results in Fig. S1. Models of mass lower than $6 M_{\odot}$ eject too little ^{26}Al to result in realistic ($1/f > 100$) dilution factors. On the other hand, models of AGB stars of masses $6 M_{\odot} - 8.5 M_{\odot}$ produce enough ^{26}Al via proton captures at the base of their hot convective envelope to result in realistic solutions (23, 35), which include ^{107}Pd and ^{182}Hf . In this case, we would have to make the assumptions that ^{53}Mn and ^{129}I came from uniform production (UP) and ^{36}Cl from *in situ* nucleosynthesis. While providing also ^{36}Cl and ^{129}I , all the supernova models overproduce ^{107}Pd and ^{182}Hf by factors from 3 to 10 of the solar abundances, as well as resulting in three orders of magnitude more ^{53}Mn than observed. This is a well known problem, which has been addressed in the past by invoking a mass cut below which the supernova material is assumed to not have been incorporated in the early solar system (18), or including mixing and fall back (36). For example, when assuming an injection mass cut at $\sim 2.1 M_{\odot}$ and $\sim 2.7 M_{\odot}$ in our $18 M_{\odot}$ and $25 M_{\odot}$ models, respectively, together with no mixing of the ejecta, we reproduce the observed $^{53}\text{Mn}/^{55}\text{Mn}$ ratio leaving all the other isotopes unchanged. In conclusion, we found potential solutions for the early solar system radioactivities when considering a single stellar polluter of mass $> 5 M_{\odot}$. This scenario comes with a series of problems, however: Stars of mass $< 10 M_{\odot}$ have evolutionary time scales

that are overly long (>30 Myr), and stars of mass $>10 M_{\odot}$ produce too much ^{53}Mn , unless a mass cut is assumed, below which the supernova material should not have been incorporated in the early solar system (18). Overall, the predicted $^{60}\text{Fe}/^{56}\text{Fe}$ are above the observed upper limit and there are O isotopic effects larger than 10% correlated to the presence of ^{26}Al , which are not observed (37, 38).

Details on the s -process production of ^{182}Hf in AGB stars and its implications

The s process in AGB stars occurs in the He-rich layer located between the He- and the H-burning shells. The $^{13}\text{C}(\alpha, n)^{16}\text{O}$ neutron source reaction is activated in the radioactive layer located below the ashes of H burning where the temperature reaches ~ 100 MK. The $^{22}\text{Ne}(\alpha, n)^{25}\text{Mg}$ neutron source reaction, instead, is activated in the convective region associated with recurrent He-burning episodes where the temperature reaches ~ 300 MK. Only AGB models of mass $\sim 3 M_{\odot}$ are significant producers of s -process ^{182}Hf in the Galaxy because in these stars the s -process is driven by the $^{13}\text{C}(\alpha, n)^{16}\text{O}$ neutron source, which generates the largest total number of neutrons of all the models and efficiently produces the heaviest s -process elements. This leads to high enhancements of ^{180}Hf , which in turn leads to high ^{182}Hf production during the secondary neutron burst generated by the $^{22}\text{Ne}(\alpha, n)^{25}\text{Mg}$ neutron source, with lower total number of neutrons but higher neutron densities than those produced by the $^{13}\text{C}(\alpha, n)^{16}\text{O}$ neutron source. In AGB stars of mass lower than $\sim 3 M_{\odot}$ the ^{22}Ne neutron source is not efficiently activated, whereas in higher mass AGB stars the ^{13}C neutron source is not efficiently activated. The four to sixfold increase in the s -process production of ^{182}Hf obtained using our new decay rate of ^{181}Hf resolves the problem highlighted by Vockenhuber *et al.* (39) and Wisshak *et al.* (40) of a non-smooth even-isotope r -process residual curve in correspondance to ^{182}W , e.g., Figure 6 of Vockenhuber *et al.* (39). The r -process residuals are calculated by subtracting from the solar abundances the s -process contributions predicted by the models (normalised to

an s -only isotope, typically ^{150}Sm (41, 42). Following this procedure, we obtain from our $3 M_{\odot}$ model a s -process contribution to ^{182}W of 74% when using our new decay rate of ^{181}Hf , as compared to a value of 60% computed with the old decay rate. This is due to the enhanced radiogenic component from the s -process ^{182}Hf , which shifts the r -process abundance of ^{182}W from 0.015 down to 0.0095 (using solar abundances normalised to $\text{Si}=10^6$), in better agreement with the neighbouring even nuclei. Over the other possible solution to this problem of decreasing the neutron-capture cross section of ^{182}W by $\sim 30\%$, our solution has the advantage of not compromising the match between the s -process AGB models and the s -process $^{182}\text{W}/^{184}\text{W}$ ratio observed in the meteoritic stardust silicon carbide (SiC) grain LU-41 that originated from an AGB star (43). This is because the $^{180}\text{Hf}/^{184}\text{W}$ ratios measured in this grain is 0.274, i.e., roughly 5 times lower than predicted by the AGB models, which means that Hf did not condense as much as W in the grain resulting in a minimal radiogenic contribution of ^{182}Hf to ^{182}W .

Discussion of the uncertainties

The times derived in Table 1 are affected by the uncertainties related to the ratios measured in early solar system. The impact of these uncertainties is, however, relatively small: roughly ± 4 Myr for $^{129}\text{I}/^{127}\text{I} = 1.19 \pm 0.20 \times 10^{-4}$ and $^{107}\text{Pd}/^{108}\text{Pd} = 5.9 \pm 2.2 \times 10^{-5}$, and ± 0.6 Myr for $^{182}\text{Hf}/^{180}\text{Hf} = 9.72 \pm 0.44 \times 10^{-5}$. For $^{247}\text{Cm}/^{235}\text{U}$, using the observed lower and upper limits of $= (1.1 - 2.4) \times 10^{-4}$ results in changes of +11 and -7 Myr, respectively. These times, as well as the UP and LE ratios, are also affected by the uncertainties related to P_{radio}/P_{stable} (in Eq. 1) and p_{radio}/p_{stable} (in Eq. 2), which depend mostly on the nuclear physics behind the s -process predictions. A conservative analysis of these uncertainties does not change the main conclusion of our study. The P_{129}/P_{127} ratio¹ suffers from the uncertainties related to the r -process residual of ^{129}Xe , the decay daughter of ^{129}I . These can be taken from Goriely (42) and result in an

¹Hereafter $P_{129}/P_{127}=P_{radio}(^{129}\text{I})/P_{stable}(^{127}\text{I})$; $p_{129}/p_{127}=p_{radio}(^{129}\text{I})/p_{stable}(^{127}\text{I})$, and so on.

uncertainty of ± 5 Myr in the UP time. The small ($\sim 10^{-4}$) $p_{129}/p_{127}(s)$ ratio does not suffer large uncertainties because the production of ^{129}I in s -process conditions is prevented by the ^{128}I nucleus having a very short half-life of ~ 25 minutes. The $p_{129}/p_{127}(r)$ ratio is derived from the r -process residuals of ^{129}Xe and ^{127}I , which mostly depend on their neutron-capture cross sections. These are given with uncertainties up to $\sim 30\%$ and $\sim 50\%$, respectively (44), which results in uncertainties in the derived r -process LE times of up to ± 14 Myr. As discussed in the paper, the $p_{182}/p_{180}(s)$ ratio depends mostly on the temperature dependence of the half-life of ^{181}Hf . When using our current lower limit (from Fig. S2, excluding the 68, 170, 298 keV states) we derive $p_{182}/p_{180}(s)=0.11$, which results in a s -process LE time of 10 Myr and 32 Myr for $\delta = 10$ and 100 Myr, respectively. The uncertainties in the $p_{182}/p_{180}(r)$ ratio mostly derive from the neutron-capture cross sections of ^{180}Hf and ^{182}W , which are up to $\sim 40\%$ each, and the magnitude of the radiogenic effect of the s -process ^{182}Hf on ^{182}W , for which we have derived above an error bar of $\sim 40\%$. These result in a uncertainty of up to ± 9 Myr in the r -process LE time. Uncertainties on the UP time are of similar size. Finally, the neutron-capture cross sections of ^{107}Pd , ^{108}Pd , and ^{107}Ag are given with maximum uncertainties of $\sim 10\%$, $\sim 25\%$, and $\sim 45\%$, respectively, which change the $p_{107}/p_{108}(s)$ ratio by $\sim 35\%$ at most, resulting in an uncertainty of up to ± 3 Myr in the s -process LE time, and of up to ± 5 Myr in the r -process LE time. Uncertainties on the UP time are of similar magnitude.

Origin of ^{26}Al , ^{36}Cl , ^{41}Ca , ^{53}Mn , and ^{60}Fe

These radioactive nuclei are lighter than those discussed in the paper and their cosmic abundances are not made by the s and r processes. Aluminum-26 is made via proton captures on ^{25}Mg , ^{36}Cl and ^{41}Ca via the capture of a neutron by ^{35}Cl and ^{40}Ca , respectively, ^{53}Mn via explosive nucleosynthesis, and ^{60}Fe via the neutron-capture chain $^{58}\text{Fe}(n,\gamma)^{59}\text{Fe}(n,\gamma)^{60}\text{Fe}$, where ^{59}Fe is unstable with a half-life of 44.51 days. When we considered a possible *supernova LE*

for the origin of ^{26}Al , ^{35}Cl , and ^{41}Ca we obtained LE times negative or lower than ~ 1 Myr. The abundances of these radioactive nuclei in the early solar system more likely resulted from self-pollution of the star forming region itself (29, 30, 31). A supernova LE for the origin of ^{53}Mn is more plausible because it results in LE times very similar to those derived for the *s*-process LE and would also produce $^{60}\text{Fe}/^{56}\text{Fe} \sim 6 \times 10^{-9}$, which is within the range observed. The isolation timescale derived from a supernova LE, however, is not robust because these nuclei can also be produced by supernovae occurring within the star-forming region.

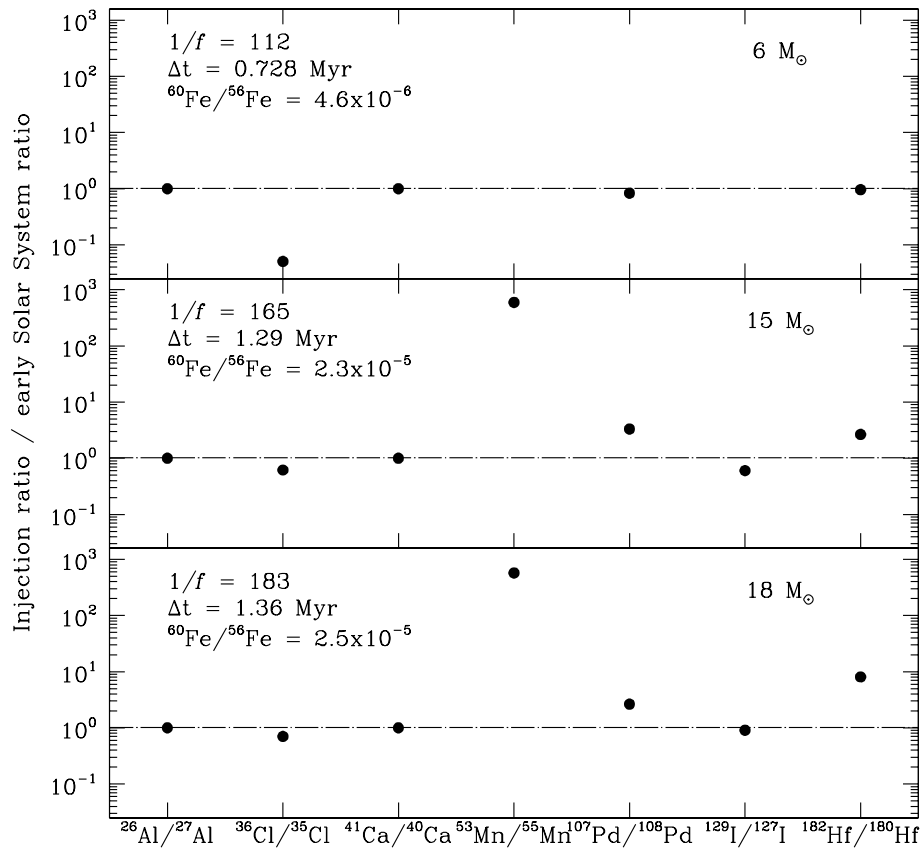


Figure S1: Results from the model that assumes injection from a single stellar source. The required dilution factor ($1/f$) and time delay (Δt) are indicated in each panel, together with the predicted $^{60}\text{Fe}/^{56}\text{Fe}$ ratio. In the $6 M_{\odot}$ model, the ratio relative to $^{129}\text{I}/^{127}\text{I}$ is offscale many orders of magnitude below unity and the ratio relative to $^{53}\text{Mn}/^{55}\text{Mn}$ is zero.

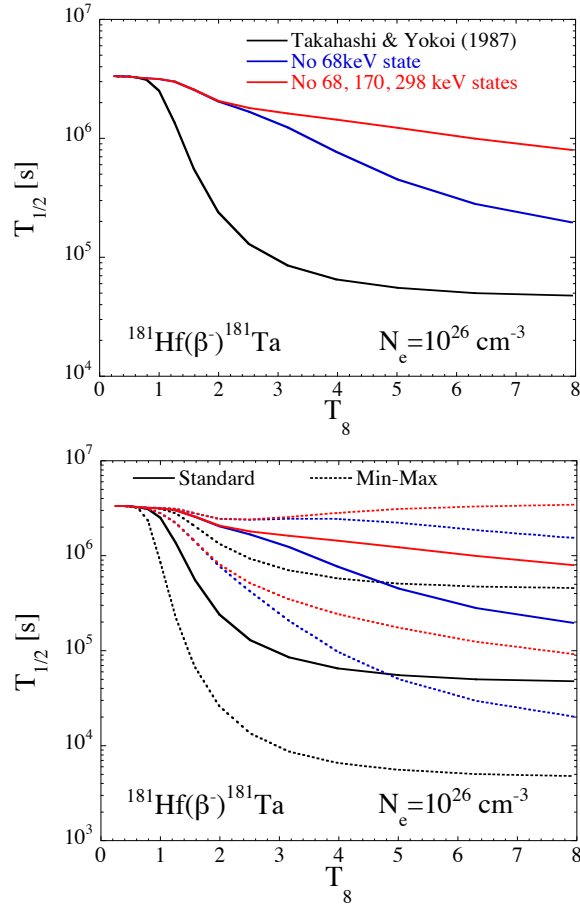


Figure S2: Three different calculations of the half-life of ^{181}Hf : same as Takahashi & Yokoi (14) (black line), same but removing the 68 keV level (blue line), and same but removing the 68 keV, 170 keV, and 298 keV levels (red line). The lower panel is the same as the upper panel, but including the minimum and maximum half-lives for each computation (dotted lines) allowed when assuming a 0.5 uncertainty on the unknown transition probabilities (42). Changing the value of the electron density N_e does not affect the results.

Table S1: Selected yields, all in units of M_{\odot} (“1.21E-07” stands for 1.21×10^{-7} and so on.)

	1.25	1.8	3	4	5	6	6.5	8	8.5
Initial stellar mass	1.25	1.8	3	4	5	6	6.5	8	8.5
Total mass ejected	0.69	1.21	2.32	3.21	4.13	5.09	5.54	6.97	7.35
²⁶ Al	1.21E-07	3.31E-07	2.19E-07	2.06E-07	4.34E-07	1.37E-06	4.09E-06	1.82E-05	3.86E-05
²⁷ Al	3.90E-05	7.04E-05	1.42E-04	1.95E-04	2.62E-04	3.18E-04	3.40E-04	4.43E-04	4.66E-04
³⁵ Cl	2.38E-06	4.20E-06	8.01E-06	1.12E-05	1.45E-05	1.78E-05	1.94E-05	2.49E-05	2.58E-05
³⁶ Cl	8.62E-10	2.26E-09	1.11E-08	9.04E-09	1.07E-08	1.08E-08	9.12E-09	1.02E-08	1.11E-08
⁴⁰ Ca	4.00E-05	7.05E-05	1.35E-04	1.89E-04	2.43E-04	2.99E-04	3.26E-04	4.18E-04	4.33E-04
⁴¹ Ca	1.54E-09	5.51E-09	2.07E-08	2.05E-08	2.60E-08	2.65E-08	1.96E-08	1.90E-08	2.56E-08
⁵³ Mn	0.00E+00								
⁵⁵ Mn	8.78E-06	1.56E-05	3.07E-05	4.17E-05	5.35E-05	6.58E-05	7.20E-05	9.24E-05	9.62E-05
⁵⁶ Fe	7.66E-04	1.35E-03	2.58E-03	3.60E-03	4.64E-03	5.72E-03	6.23E-03	7.80E-03	8.30E-03
⁶⁰ Fe	3.15E-07	2.82E-07	2.83E-08	5.30E-07	2.23E-06	3.83E-06	4.31E-06	6.43E-06	5.18E-06
¹⁰⁷ Pd	4.82E-11	2.04E-09	8.06E-09	3.46E-09	8.40E-12	1.19E-11	5.03E-11	5.74E-11	1.09E-10
¹⁰⁸ Pd	9.70E-10	1.44E-08	5.75E-08	2.68E-08	4.11E-09	5.07E-09	5.61E-09	7.12E-09	7.33E-09
¹²⁷ I	2.42E-09	8.19E-09	2.25E-08	1.88E-08	1.43E-08	1.77E-08	1.91E-08	2.45E-08	2.32E-08
¹²⁹ I	1.53E-16	4.61E-14	5.98E-12	5.36E-12	2.03E-14	2.76E-14	5.15E-14	4.44E-14	1.46E-13
¹⁸⁰ Hf	1.77E-10	5.27E-09	1.63E-08	8.53E-09	1.07E-09	1.32E-09	1.43E-09	1.82E-09	1.89E-09
¹⁸² Hf	1.82E-12	1.06E-10	2.46E-09	2.42E-09	1.90E-11	1.77E-11	1.18E-11	9.68E-12	7.62E-12

Table S1: continues.

	Initial stellar mass	12	15	18	25	Solar system
Total mass ejected	10.6	13.3	16.3	23.1	mass fraction	
²⁶ Al	9.32E-06	2.21E-05	3.20E-05	6.54E-05		
²⁷ Al	1.58E-03	3.83E-03	7.05E-03	1.49E-02		5.65E-05
³⁵ Cl	9.39E-05	1.78E-04	3.75E-04	2.27E-03		3.50E-06
³⁶ Cl	7.70E-07	1.71E-06	3.10E-06	2.66E-05		
⁴⁰ Ca	3.52E-03	5.73E-03	7.83E-03	1.33E-02		5.88E-05
⁴¹ Ca	2.28E-06	4.58E-06	9.78E-06	5.89E-05		
⁵³ Mn	9.26E-05	1.34E-04	1.76E-04	2.22E-04		
⁵⁵ Mn	5.39E-04	8.30E-04	1.05E-03	1.24E-03		1.29E-05
⁵⁶ Fe	8.26E-02	1.41E-01	1.54E-01	1.59E-01		1.12E-03
⁶⁰ Fe	3.25E-05	9.08E-05	1.36E-04	1.14E-04		
¹⁰⁷ Pd	2.54E-10	4.90E-10	5.31E-10	1.26E-09		
¹⁰⁸ Pd	1.03E-08	1.27E-08	1.54E-08	2.35E-08		9.92E-10
¹²⁷ I	3.39E-08	4.07E-08	4.70E-08	6.16E-08		3.50E-09
¹²⁹ I	3.36E-10	5.97E-10	1.22E-09	1.44E-09		
¹⁸⁰ Hf	2.69E-09	3.44E-09	4.54E-09	6.04E-09		2.52E-10
¹⁸² Hf	1.31E-10	1.61E-10	6.64E-10	1.18E-09		

Table S2: Radioisotopes of potential stellar origin in the early solar system. τ is the mean life time of each isotope in Myr. In the case of ^{247}Cm also the reference isotope ^{235}U is radioactive, with $\tau = 1020$ Myr. The early solar system ratios are taken from Dauphas & Chaussidon (5), except for $^{41}\text{Ca}/^{40}\text{Ca}$, which is updated according to Liu *et al.* (45), $^{247}\text{Cm}/^{235}\text{U}$ reported directly from Brennecka *et al.* (33), and $^{60}\text{Fe}/^{56}\text{Fe}$, which is currently debated and for which we give the range discussed in detail by Mishra, Chaussidon & Marhas (46).

Isotope	$\tau(\text{Myr})$	Reference isotope	Early solar system ratio
^{247}Cm	22.5	^{235}U	$(1.1 - 2.4) \times 10^{-4}$
^{129}I	23	^{127}I	$(1.19 \pm 0.20) \times 10^{-4}$
^{182}Hf	13	^{180}Hf	$(9.72 \pm 0.44) \times 10^{-5}$
^{107}Pd	9.4	^{108}Pd	$(5.9 \pm 2.2) \times 10^{-5}$
^{53}Mn	5.3	^{55}Mn	$(6.28 \pm 0.66) \times 10^{-6}$
^{60}Fe	3.8	^{56}Fe	$10^{-9} - 10^{-6}$
^{26}Al	1.03	^{27}Al	$(5.23 \pm 0.13) \times 10^{-5}$
^{36}Cl	0.43	^{35}Cl	$(17.2 \pm 2.5) \times 10^{-6}$
^{41}Ca	0.15	^{40}Ca	$\sim 4.2 \times 10^{-9}$